D. Gurešić[1], A. Đorđević[1], A. Marković[1], M. Tomović[1], N. Talijan[2], I. Manasijević[3]

DOI: 10.7251/JEPMEN1608045G

UDK: 552.527:543.4

Scientific paper

EFECTS OF CHEMICAL COMPOSITION ON THE MICROSTRUCTURE AND PROPERTIES OF THE CU-Ge-Sb ALLOYS

Dejan Gurešić[1], Aleksandar Đorđević[1], Aleksandar Marković[1], Milica Tomović[1], Nadežda Talijan[2], Ivana Manasijević[3]

coadjordjevic90@gmail.com

[1]*Faculty of Technical Science, University in Priština, kosovska Mitrovica*

[2]*Institute of Chemistry Technology and Metallurgy, Belgrade, RS*

[3]*Technical Faculty, University in Belgrade, Bor, RS*

Abstract

In the current study a ternary Cu-Ge-Sb system has been experimentally assessed. Chemical and phase compositions of the alloy samples from three vertical sections Cu-GeSb, Ge-CuSb and Sb-CuGe were studied using scanning electron microscopy (SEM) and energy dispersive spectroscopy (EDS) and confirmed by X-ray diffraction analysis (XRD). Hardness of the alloys was measured by Brinell method while hardness of phases was measured using micro Vickers method. Electrical conductivity of the studied alloys was measured using eddy current instrument. Based on experimentally determined values iso-lines of hardness and electrical conductivity for the whole ternary system were calculated using assumed mathematical models.

Key words: *ternary Cu-Ge-Sb system, microstructural investigation, hardness test, electrical conductivity*

1. INTRODUCTION

In recent years there has been a lot of interest in investigation of binary and ternary Ge alloys [1-3]. Germanium based alloys are extensively studied because of their semiconducting properties and applications in the electronic industry [4-6]. Binary Cu-Ge alloys have excellent physical and chemical properties, such as low room-temperature resistance and high thermal stability, which are potentially useful in the optical and electronic devices [7-10]. Furthermore, Ge and Sb based systems are of importance for the development of phase-change materials (PCM) [11-13] which have a wide application in the modern information storage technology for making optical discs, DVD, Blue-Ray discs and flash memories [14,15]. Over the past few decades ternary alloys based on Cu-Ge-X (X=Au, Ag, …) [16,17] and Ge-Sb-X, (X=Bi, Ag, In, …) [18-20] have also been attracting significant interest as semiconductor materials. However, to the best of our knowledge the system that is a combination of Cu with Ge and Sb in different ratios has not been investigated up to now. The aim of this study was experimental investigation of the alloys from a ternary Cu-Ge-Sb system in terms of their

microstructure, phase composition, hardness and electrical conductivity. Based on experimentally determined values iso-lines of hardness and electrical conductivity for the whole ternary system were calculated using assumed mathematical models. The presented results can be basis for further investigations given that the ternary Cu-Ge-Sb system has not yet been studied from this point of view in literature.

2. EXPERIMENTAL PROCEDURE

Studied alloy samples from the ternary Cu-Ge-Sb system weighing about 3 g were prepared from high purity (99.999 at. %) elements. The samples were initially melted in an induction furnace under inert (Ar) atmosphere with the determined average weight loss of about 1 at. %. Given that Sb is highly volatile an additional amount of Sb (about 1 to 2 at. %) was added to compensate for the weight loss. The obtained alloy samples were then characterized in terms of their structure and phase composition by light optical microscopy (LOM) using OLYMPUS GX41 inverted optical microscope, as well as by scanning electron microscopy (SEM) combined with energy dispersive spectroscopy (EDS) using JEOL (JSM6460) scanning electron microscope equipped with Oxford Instruments X-act energy dispersive spectrometer and by X-ray diffraction analysis (XRD) using Bruker D2 PHASER powder diffractometer with Cu tube (KFLCu-2K). The obtained X-ray patterns were subsequently analyzed using Topas 4.2 software and ICDD databases PDF2 (2013). Hardness of the alloy samples was measured by Brinell test using Innovatest Nexus 3001 hardness tester by applying force of 294.2 N for a loading time of 15 s, while hardness of the present phases was measured by Vickers test using digital micro-hardness tester DHV-1000 with an applied force of 0.245 N and 15 s loading time. Electrical conductivity of the prepared alloy samples was measured using eddy current instrument Foerster SIGMATEST 2.069.

3. LITERATURE DATA

Considering that, to our knowledge, no studies on the ternary Cu-Ge-Sb system can be found in literature, thermodynamic assessment was based on already well-known binary sub-systems (Cu-Ge [21], Ge-Sb [22] and Cu-Sb [23]). A list of phases that are possibly present in the studied ternary system and their crystallographic data are given in Table 1.

Table 1. Considered phases and their crystal structures

Phase common name	Space group symbol	Pearson's symbol
L	-	-
(Sb)	$R\bar{3}m$	*hR*2
(Ge)	$Fd\bar{3}m$	*cF*8
(Cu)	$Fm\bar{3}m$	*cF*4
β	$Fm\bar{3}m$	*cF*16
γ($Cu_{85}Sb_{15}$)	*P6₃/mmc*	*hP*2
δ(Cu_4Sb)	*P6₃/mmc*	*hP?*
ε(Cu_3Sb)	*Pmmn*	*oP*8
ζ($Cu_{77}Sb_{23}$)	$p\bar{3}$	*hP*26
η(Cu_2Sb)	*P4/nmm*	*tP*6
ε' ($Cu_{0.765}Ge_{0.235}$)		
η' (Cu_3Ge)	*Pmnm*	*oP8*
θ ($Cu_{0.735}Ge_{0.265}$)	$Im\bar{3}m$	*cI2*
ξ (Cu_5Ge)	*P6₃/mmc*	*hP2*

4. RESULTS AND DISCUSSION

In order to observe changes of properties of the alloys with changes of their composition, the samples from the three selected vertical sections were studied using the same experimental techniques.

4.1. Vertical section Ge-CuSb

Nine ternary alloy samples were selected for investigation of Ge-CuSb vertical section. The Ge content in the prepared alloy samples increases from the sample 1 to the sample 9 for approximately 10 at. % between each consecutive sample.

D. Gurešić[1], A. Đorđević[1], A. Marković[1], M. Tomović[1], N. Talijan[2], I. Manasijević[3]

The alloy sample with number 1 has the lowest Ge content while the sample 9 has the highest Ge content compared to the all other samples. Contents of Cu and Sb were always kept at approximately same 50:50 ratio. In this way it was possible to observe changes of properties and microstructure of the CuSb alloys with addition of Ge. The binary CuSb alloy with 50:50 composition consists of two phases (Sb)+ η(Cu_2Sb). Identified phases in the studied ternary alloys and their experimentally determined compositions are given in Table 2. According to the results present in Table 2, the same phases were detected phases in the all nine ternary samples. Addition of Ge did not result in a change of (Sb) and η(Cu_2Sb) phases and the added Ge just formed the third phase solid solution (Ge). Experimentally determined maximum solubility of Ge in solid solution (Sb) and intermetallic compound η(Cu_2Sb) is 0.55 at. %. Also, solid solution of (Ge) can dissolve small amounts of Sb and Cu. The maximal detected solubility of Sb is 0.95 at.% and of Cu is 0.87 at. %. Detected solubility of Sb in η(Cu_2Sb) phase, Sb and Cu in solid solution (Ge) and Cu and Ge in solid solution (Sb) were neglected because they were less than 1 at. % in each phase. SEM micrograph of a microstructure of the sample 5 is presented on Figure 1. On the presented micrograph (Fig. 1) three phases are visible. Solid solution (Ge) appears as a dark phase, solid solution (Sb) is white phase, while the third detected phase is gray. The same samples were investigated using XDR analysis and obtained results are given in Table 3. The experimentally determined phase composition by SEM-EDS technique was confirmed by XRD analysis using Rietveld method. In addition to confirmation of composition, lattice parameters of the determined phases were obtained. The calculated lattice parameters are given in Table 3 together with the literature values. Literature data for (Ge) solid solution were taken from Morozkin [24]. The calculated values of the lattice parameters from the current study were found to be in a same range as the reported values a=b=c=5.6522 Å [24]. The determined lattice parameters for solid solution (Sb) are consistent with data reported by Li et al. [25], while the obtained lattice parameters for intermetallic compound η(Cu_2Sb) from this study were also found to be in the same range as the values a=b=3.97 Å and c=6.06 given by Reshak et al. [26]. The recorded XRD pattern of the alloy sample 9 is presented on Figure 2.

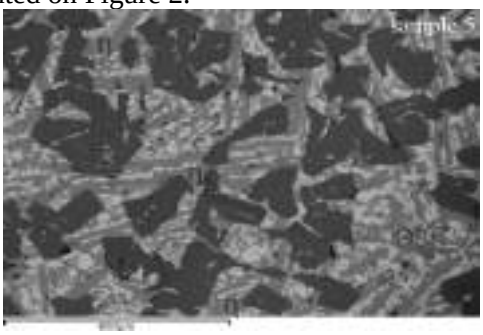

Figure 1. Microstructure of the sample 5 analyzed by the SEM-EDS technique

In addition, the samples were further observed using light optical microscopy. Micrographs of microstructures of the samples 1, 2, 6 and 8 are presented on Figure 3. Three phases are visible in the all studied samples. With an increasing Ge content, phase rich with germanium solid solution (Ge) is becoming dominant in the microstructures. In the alloy sample 1, Ge content is 9.98 at. % and the very small region of (Ge) phase is visible in its microstructure, while (Sb) and η(Cu_2Sb) phases are dominant. In contrast, quite opposite can be observed on the micrograph of the sample 8. Content of Ge in sample 8 is 80.34 at. % and solid solution (Ge) phase is dominant.

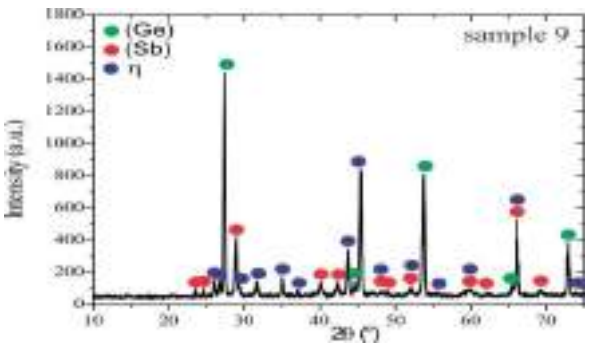

Figure 2. XRD pattern of the sample

D. Gurešić[1], A. Đorđević[1], A. Marković[1], M. Tomović[1], N. Talijan[2], I. Manasijević[3]

Table 2. Experimentally determined compositions of alloy samples and phases from Ge-CuSb vertical section

Sample	Overall composition (at.%)	Experiment. Determined phases	Compositions of phases (at.%)		
			Cu	Ge	Sb
			exp.	exp.	exp.
1	44.78 Cu 9.98 Ge 45.24 Sb	(Ge) (Sb) η(Cu_2Sb)	0.13±0.2 0.08±0.3 67.15±0.1	99.52±0.3 0.53±0.4 0.03±0.2	0.35±0.1 99.39±0.4 32.82±0.4
2	40.05 Cu 20.17 Ge 39.78 Sb	(Ge) (Sb) η(Cu_2Sb)	0.08±0.3 0.56±0.4 68.02±0.2	98.98±0.1 0.17±0.5 0.43±0.3	0.94±0.3 99.27±0.3 31.55±0.4
3	35.15 Cu 29.98 Ge 34.87 Sb	(Ge) (Sb) η(Cu_2Sb)	0.54±0.2 0.18±0.2 67.54±0.3	99.01±0.4 0.09±0.6 0.13±0.1	0.45±0.3 99.73±0.1 32.33±0.1
4	30.21 Cu 39.89 Ge 29.90 Sb	(Ge) (Sb) η(Cu_2Sb)	0.36±0.1 0.15±0.5 67.71±0.1	98.89±0.3 0.13±0.2 0.54±0.2	0.75±0.3 99.72±0.2 31.75±0.4
5	24.79 Cu 50.06 Ge 25.15 Sb	(Ge) (Sb) η(Cu_2Sb)	0.87±0.2 0.23±0.2 67.98±0.2	98.54±0.1 0.09±0.4 0.13±0.5	0.59±0.4 99.68±0.4 31.89±0.1
6	20.09 Cu 60.13 Ge 19.78 Sb	(Ge) (Sb) η(Cu_2Sb)	0.05±0.4 0.18±0.4 67.09±0.2	99.56±0.3 0.55±0.1 0.15±0.1	0.39±0.3 99.27±0.4 32.76±0.5
7	14.60 Cu 69.97 Ge 15.43 Sb	(Ge) (Sb) η(Cu_2Sb)	0.66±0.3 0.15±0.1 68.03±0.1	98.71±0.4 0.42±0.4 0.34±0.2	0.63±0.3 99.43±0.7 31.63±0.6
8	9.68 Cu 80.34 Ge 9.98 Sb	(Ge) (Sb) η(Cu_2Sb)	0.02±0.3 0.87±0.1 68.16±0.3	99.03±0.3 0.38±0.5 0.54±0.6	0.95±0.2 98.75±0.3 31.30±0.5
9	5.10 Cu 89.87 Ge 5.03 Sb	(Ge) (Sb) η(Cu_2Sb)	0.34±0.5 0.56±0.1 68.09±0.2	98.79±0.3 0.54±0.5 0.14±0.4	0.87±0.3 98.90±0.1 31.77±0.1

D. Gurešić[1], A. Đorđević[1], A. Marković[1], M. Tomović[1], N. Talijan[2], I. Manasijević[3]

Table 3. The results of XRD analysis: identified phases and calculated lattice parameters compared with literature data

S.	Coexisting phases		Lattice parameters (Å)			
	SEM-EDS	XRD	*a=b*		*c*	
			Exp.	Ref.	Exp.	Ref.
1	(Ge) (Sb) η(Cu_2Sb)	(Ge) (Sb) η(Cu_2Sb)	5.6534(1) 4.3087(5) 3.9786(1)	5.6522[24] 4.30724[25] 3.97[26]	11.2765(6) 6.0687(1)	11.2754[25] 6.06[26]
2	(Ge) (Sb) η(Cu_2Sb)	(Ge) (Sb) η(Cu_2Sb)	5.6576(1) 4.3065(1) 3.9786(5)	5.6522[24] 4.30724[25] 3.97[26]	11.2787(5) 6.0687(7)	11.2754[25] 6.06[26]
3	(Ge) (Sb) η(Cu_2Sb)	(Ge) (Sb) η(Cu_2Sb)	5.6534(3) 4.3098(9) 3.9789(1)	5.6522[24] 4.30724[25] 3.97[26]	11.2756(4) 6.0687(3)	11.2754[25] 6.06[26]
4	(Ge) (Sb) η(Cu_2Sb)	(Ge) (Sb) η(Cu_2Sb)	5.6576(6) 4.3066(6) 3.9766(8)	5.6522[24] 4.30724[25] 3.97[26]	11.2765(5) 6.0687(5)	11.2754[25] 6.06[26]
5	(Ge) (Sb) η(Cu_2Sb)	(Ge) (Sb) η(Cu_2Sb)	5.6534(2) 4.3057(6) 3.9756(2)	5.6522[24] 4.30724[25] 3.97[26]	11.2756(6) 6.0655(2)	11.2754[25] 6.06[26]
6	(Ge) (Sb) η(Cu_2Sb)	(Ge) (Sb) η(Cu_2Sb)	5.6576(2) 4.3087(8) 3.9777(1)	5.6522[24] 4.30724[25] 3.97[26]	11.2786(6) 6.0656(3)	11.2754[25] 6.06[26]
7	(Ge) (Sb) η(Cu_2Sb)	(Ge) (Sb) η(Cu_2Sb)	5.6554(4) 4.3056(5) 3.9745(6)	5.6522[24] 4.30724[25] 3.97[26]	11.2786(5) 6.0687(9)	11.2754[25] 6.06[26]
8	(Ge) (Sb) η(Cu_2Sb)	(Ge) (Sb) η(Cu_2Sb)	5.6544(1) 4.3097(8) 3.9788(3)	5.6522[24] 4.30724[25] 3.97[26]	11.2756(3) 6.0687(7)	11.2754[25] 6.06[26]
9	(Ge) (Sb) η(Cu_2Sb)	(Ge) (Sb) η(Cu_2Sb)	5.6534(7) 4.3098(5) 3.9788(3)	5.6522[24] 4.30724[25] 3.97[26]	11.2765(5) 6.0652(3)	11.2754[25] 6.06[26]

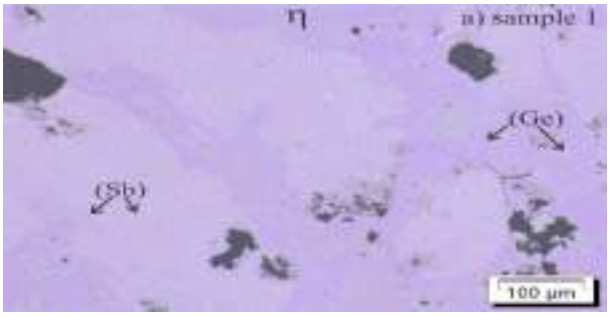

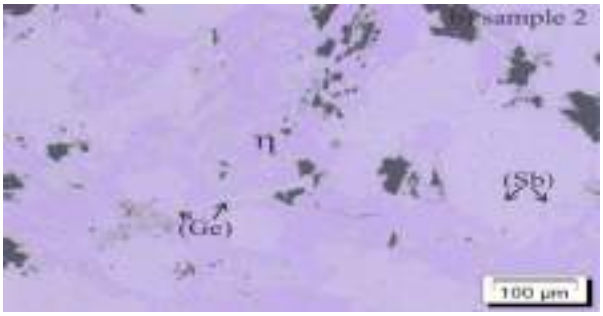

D. Gurešić[1], A. Đorđević[1], A. Marković[1], M. Tomović[1], N. Talijan[2], I. Manasijević[3]

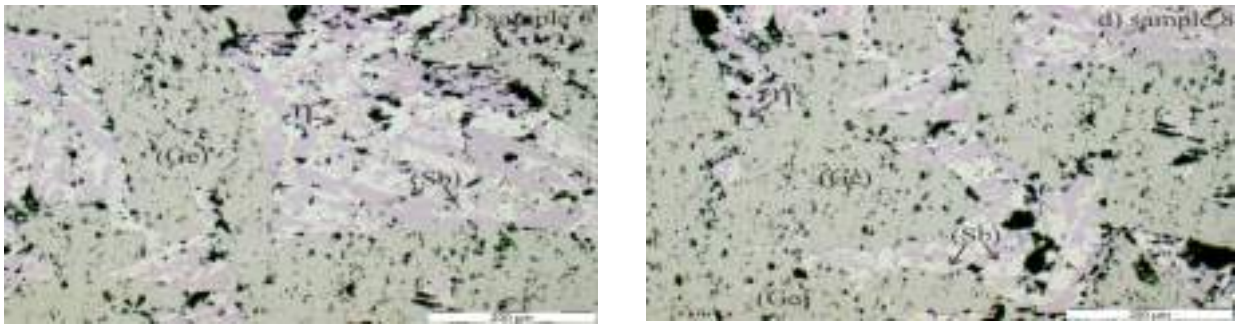

Figure 3. Microstructures of the selected alloy samples observed with LOM

Vickers hardness of the phases identified in the microstructures was measured and in Table 4 are given average values from all measurements. Hardness of the same phases in the each sample was measured minimum five times at different parts of the sample. Therefore, the values given in Table 4 represent an average from at least 45 measurements (nine samples and five measurements per same phase per sample).

Table 4. Measured Vickers micro-hardness of the phases in ternary Cu-Ge-Sb system

Vickers test	Determined phase		
	(Ge)	(Sb)	η(Cu_2Sb)
hardness (MN/m^2)	857.13	318.52	469.54

It was found that the solid solution (Ge) has the highest value of hardness 857.13 MN/m^2 while intermetallic compound η(Cu_2Sb) and solid solution (Sb) have the lowest values.

Hardness of the samples was investigated using Brinell test and the measured values are given in Table 5. Measurements were carried out in three points for each sample. In order to illustrate behavior of hardness of the ternary alloys in Table 5 are added values for one binary CuSb alloy and pure Ge. Graphical presentation of a dependence of Brinell hardness vs Ge mole fraction is given on Figure 4. According to the obtained results for the ternary alloys, values of hardness have a trend of decreasing with an addition of Ge up to alloy $Ge_{60.13}Cu_{20.09}Sb_{19.78}$. From this point, further addition of Ge results in a change of the trend and hardness starts to increase with addition of Ge.

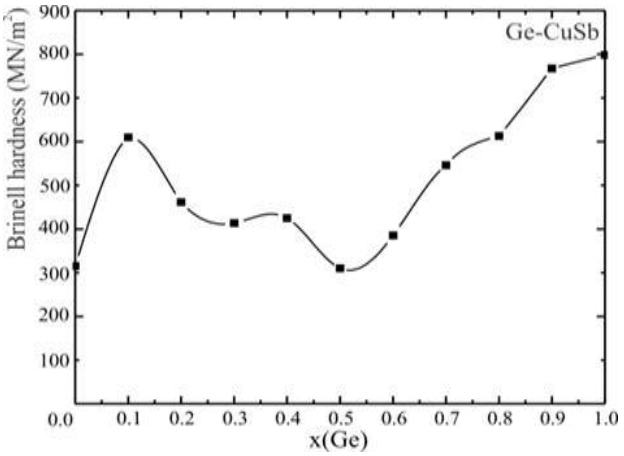

Figure 4. Graphical presentation of the Brinell hardness of the samples from the Ge-CuSb vertical section

Electrical conductivity of the studied samples from the Ge-CuSb vertical section was measured in four points for each alloy. The experimentally measured values together with calculated mean values are given in Table 6. Literature value of electrical conductivity of pure Ge (0.002 MS/m) was taken from [27]. The obtained results for ternary alloys (Table 6) show small values of electrical conductivity in range 0.3695 to 3.052 MS/m.

D. Gurešić[1], A. Đorđević[1], A. Marković[1], M. Tomović[1], N. Talijan[2], I. Manasijević[3]

Table 5. Brinell hardness of the alloys of the samples from the Ge-CuSb vertical section

Sample	Mole fraction of components			Brinell hardness (MN/m^2)			
				Value for different measurement			Mean value
	x(Ge)	x(Sb)	x(Cu)	1	2	3	
Bin. 1	0	0.50	0.50	315.5	316.4	313.3	315.1
1	**0.10**	0.45	0.45	612.9	609.5	606.8	609.7
2	**0.20**	0.40	0.40	462.9	458.3	463.1	461.4
3	**0.30**	0.35	0.35	412.7	413.3	414.6	413.5
4	**0.40**	0.30	0.30	423.8	425.9	424.9	424.9
5	**0.50**	0.25	0.25	313.6	307.6	309.6	310.3
6	**0.60**	0.20	0.20	385.5	383.8	386.7	385.3
7	**0.70**	0.15	0.15	550.3	544.5	543.6	546.1
8	**0.80**	0.10	0.10	614.54	612.3	612.5	613.1
9	**0.90**	0.05	0.05	769.1	767.5	766.5	767.7
Ge	**1.00**	0	0	798.1	798.3	798.6	798.3

It can be observed that the electrical conductivity of ternary alloys is decreasing with an addition of Ge, which can be explained by reduction of Cu content in the studied alloys. Graphical presentation of the dependence of electrical conductivity from Ge mole fraction is given on Figure 5. It can be seen that the samples 1 and 2 have similar values of the electrical conductivity while starting from the sample 3 values of electrical conductivity decrease significantly.

Table 6. Electrical conductivity of the alloys from the Ge-CuSb vertical section

Sample	Mole fraction of components			Electrical conductivity (MS/m)				
				Value for different measurement				Mean value
	x(Ge)	x(Sb)	x(Cu)	1	2	3	4	
Bin. 1	0	0.5	0.5	3.897	3.894	3.889	3.892	3.893
1	0.1	0.45	0.45	3.018	3.100	3.076	3.015	3.052
2	0.2	0.4	0.4	2.795	2.791	2.729	2.758	2.768
3	0.3	0.35	0.35	1.125	1.151	1.145	1.134	1.139
4	0.4	0.3	0.3	0.825	0.820	0.834	0.838	0.829
5	0.5	0.25	0.25	0.767	0.776	0.780	0.776	0.775
6	0.6	0.2	0.2	0.652	0.678	0.617	0.628	0.644
7	0.7	0.15	0.15	0.523	0.524	0.521	0.523	0.523
8	0.8	0.1	0.1	0.432	0.438	0.433	0.434	0.434
9	0.9	0.05	0.05	0.365	0.376	0.369	0.368	0.369
Ref. [27]	1	0	0					0.002

D. Gurešić[1], A. Đorđević[1], A. Marković[1], M. Tomović[1], N. Talijan[2], I. Manasijević[3]

4.2. Vertical section Sb-CuGe

Changes in microstructures, electrical and mechanical properties with increasing amount of Sb of the alloy samples from vertical section Sb-CuGe were studied. The contents of Cu and Ge were in kept at constant ratio. As in previous case, nine alloy samples from the vertical section were investigated and they were marked with numbers from 10 to 18. Experimentally determined compositions of the samples and phases identified in the studied samples from Sb-CuGe vertical section are given in Table 7. Only in the sample 10 with 10.08 at. % of Sb, (Ge), η(Cu_2Sb) and η'(Cu_3Ge) phases were detected, in all other samples (samples 11 to 18) the same phases as in the samples from the Ge-CuSb vertical section were detected. The determined compositions of the phases are very close to their theoretical compositions as the differences are less than 1 at. %. The effect of element which is not theoretically present in a phase was neglected. SEM micrograph of the sample 10 is given on Figure 6 as an example. In the presented microstructure (Figure 6) solid solution (Ge) appears as a dark oval phase, while intermetallic compounds η(Cu_2Sb) and η'(Cu_3Ge) appear somewhat brighter. The phase compositions determined by EDS analysis were additionally checked using XRD analysis. The obtained results of XRD analysis are given in Table 8. The results of XRD analysis confirm presence of the all phases detected by EDS. Besides phase composition in Table 8 are also given determined lattice parameters for the detected phases compared with literature data [24-26]. The observed differences between the determined and the literature values of parameters are in the third digit after the decimal point, which is reasonable. When compared, the determined values of lattice parameters for the η'(Cu_3Ge) phase were found to be in a close agreement with data given by Caspi et al. [28]. LOM micrographs illustrating microstructures of the four studied alloy samples (11, 14, 15 and 18) are given on Figure 7.

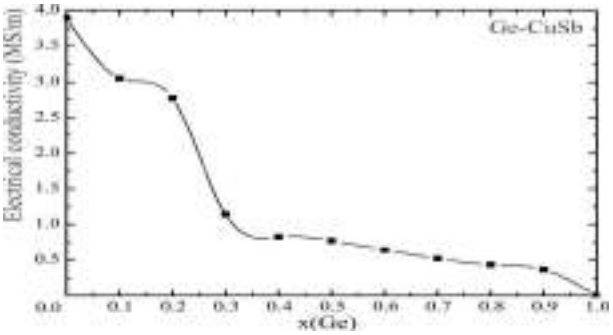

Figure 5. Electrical conductivity of the investigated alloy samples from the Ge-CuSb vertical section

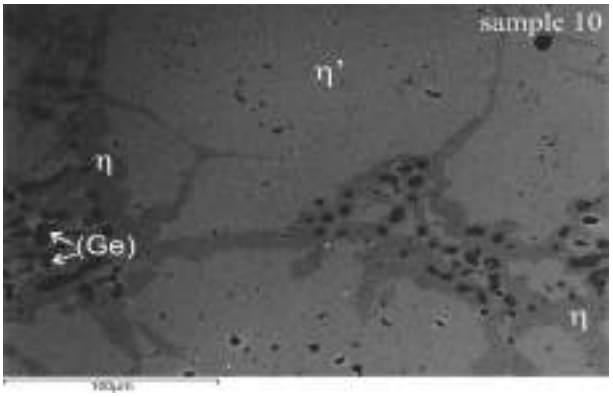

Figure 6. Microstructure of the sample 10 analyzed using SEM-EDS technique

D. Gurešić[1], A. Đorđević[1], A. Marković[1], M. Tomović[1], N. Talijan[2], I. Manasijević[3]

Table 7. Experimentally determined compositions of the samples and phases from Sb-CuGe vertical section

Sample	Overall composition (at.%)	Experiment. Determined phases	Compositions of phases (at.%)		
			Cu	Ge	Sb
			exp.	exp.	exp.
10	44.74 Cu 45.18 Ge 10.08 Sb	(Ge) η(Cu_2Sb) η'(Cu_3Ge)	0.54±0.5 66.98±0.2 74.67±0.3	98.75±0.1 0.13±0.3 25.01±0.4	0.71±0.3 32.89±0.5 0.32±0.3
11	39.87 Cu 39.98 Ge 20.15Sb	(Ge) (Sb) η(Cu_2Sb)	0.25±0.5 0.67±0.8 66.33±0.2	99.16±0.2 0.13±0.8 0.03±0.3	0.59±0.3 99.20±0.8 33.64±0.1
12	34.32 Cu 35.54 Ge 30.14 Sb	(Ge) (Sb) η(Cu_2Sb)	0.65±0.8 0.13±0.3 67.02±0.5	99.05±0.5 0.32±0.2 0.18±0.2	0.30±0.2 99.55±0.2 32.80±0.3
13	28.99 Cu 30.56 Ge 40.45 Sb	(Ge) (Sb) η(Cu_2Sb)	0.45±0.5 0.34±0.4 67.15±0.2	98.96±0.8 0.29±0.4 0.54±0.3	0.59±0.5 99.37±0.1 32.31±0.1
14	24.66 Cu 24.67 Ge 50.67 Sb	(Ge) (Sb) η(Cu_2Sb)	0.17±0.3 0.54±0.3 67.54±0.1	99.03±0.1 0.54±0.3 0.65±0.8	0.80±0.7 98.92±0.2 31.81±0.3
15	20.24 Cu 19.98 Ge 59.78 Sb	(Ge) (Sb) η(Cu_2Sb)	0.45±0.5 0.49±0.2 67.56±0.8	98.78±0.8 0.38±0.7 0.54±0.1	0.77±0.8 99.13±0.2 31.90±0.3
16	14.99 Cu 14.94 Ge 70.07 Sb	(Ge) (Sb) η(Cu_2Sb)	0.76±0.2 0.09±0.3 67.52±0.3	99.05±0.8 0.52±0.1 0.35±0.1	0.19±0.2 99.39±0.3 32.13±0.5
17	10.02 Cu 10.01 Ge 79.97 Sb	(Ge) (Sb) η(Cu_2Sb)	0.98±0.8 0.17±0.2 66.52±0.2	98.65±0.7 0.72±0.1 0.15±0.1	0.37±0.1 99.11±0.3 33.33±0.2
18	4.36 Cu 4.97 Ge 90.67 Sb	(Ge) (Sb) η(Cu_2Sb)	0.66±0.4 0.56±0.3 66.98±0.1	98.67±0.5 0.13±0.8 0.53±0.3	0.67±0.4 99.31±0.3 32.49±0.8

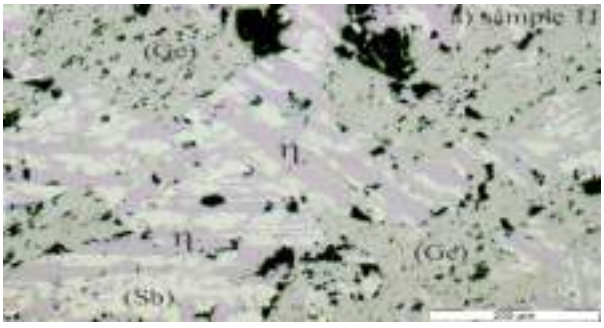

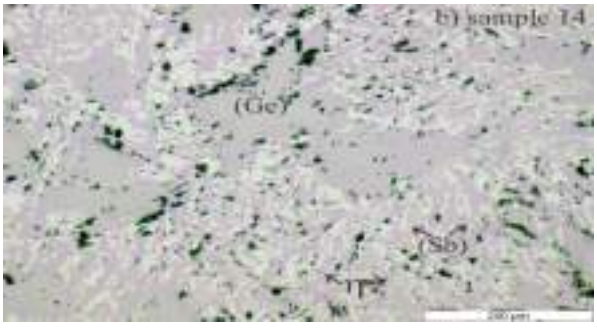

D. Gurešić[1], A. Đorđević[1], A. Marković[1], M. Tomović[1], N. Talijan[2], I. Manasijević[3]

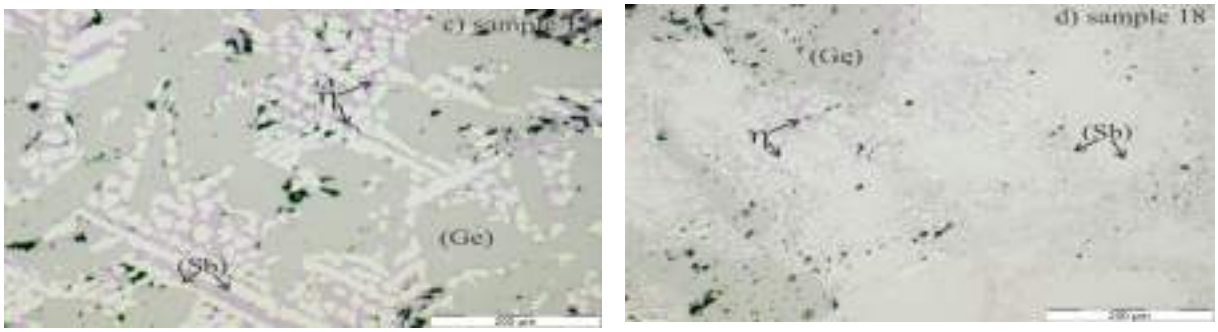

Figure 7. Microstructures of the selected alloy samples observed with LOM

Table 8. Results of XRD analysis: identified phases and calculated lattice parameters compared with literature data

S.	Coexisting phases		Lattice parameters (Å)					
	SEM-EDS	XRD	a		b		c	
			Exp.	Ref.	Exp.	Ref.	Exp.	Ref.
10	(Ge) η(Cu_2Sb) η'(Cu_3Ge)	(Ge) η(Cu_2Sb) η'(Cu_3Ge)	5.6587(2) 3.9787(1) 5.2786(9)	5.6522[24] 3.97[26] 5.272[28]	4.2098(2)	4.204[28]	6.0698(5) 4.5756(2)	6.06[26] 4.578[28]
11	(Ge) (Sb) η(Cu_2Sb)	(Ge) (Sb) η(Cu_2Sb)	5.65687(2) 4.3076(3) 3.9788(8)	5.6522[24] 4.30724[25] 3.97[26]			11.2756(3) 6.0698(2)	11.2754[25] 6.06[26]
12	(Ge) (Sb) η(Cu_2Sb)	(Ge) (Sb) η(Cu_2Sb)	5.6598(7) 4.3097(5) 3.9786(5)	5.6522[24] 4.30724[25] 3.97[26]			11.2756(5) 6.0678(3)	11.2754[25] 6.06[26]
13	(Ge) (Sb) η(Cu_2Sb)	(Ge) (Sb) η(Cu_2Sb)	5.6546(2) 4.3098(8) 3.9789(2)	5.6522[24] 4.30724[25] 3.97[26]			11.2796(7) 6.0676(5)	11.2754[25] 6.06[26]
14	(Ge) (Sb) η(Cu_2Sb)	(Ge) (Sb) η(Cu_2Sb)	5.6587(3) 4.3098(6) 3.9786(2)	5.6522[24] 4.30724[25] 3.97[26]			11.2786(3) 6.0687(3)	11.2754[25] 6.06[26]
15	(Ge) (Sb) η(Cu_2Sb)	(Ge) (Sb) η(Cu_2Sb)	5.6537(3) 4.3078(3) 3.9778(2)	5.6522[24] 4.30724[25] 3.97[26]			11.2785(4) 6.0687(3)	11.2754[25] 6.06[26]
16	(Ge) (Sb) η(Cu_2Sb)	(Ge) (Sb) η(Cu_2Sb)	5.6537(3) 4.3098(7) 3.9786(3)	5.6522[24] 4.30724[25] 3.97[26]			11.2756(6) 6.0678(4)	11.2754[25] 6.06[26]
17	(Ge) (Sb) η(Cu_2Sb)	(Ge) (Sb) η(Cu_2Sb)	5.6598(8) 4.3098(7) 3.9746(3)	5.6522[24] 4.30724[25] 3.97[26]			11.2786(3) 6.0687(9)	11.2754[25] 6.06[26]
18	(Ge) (Sb) η(Cu_2Sb)	(Ge) (Sb) η(Cu_2Sb)	5.6589(5) 4.3049(2) 3.9746(5)	5.6522[24] 4.30724[25] 3.97[26]			11.2764(3) 6.0624(3)	11.2754[25] 6.06[26]

D. Gurešić[1], A. Đorđević[1], A. Marković[1], M. Tomović[1], N. Talijan[2], I. Manasijević[3]

Three phases at a time were observed using LOM within microstructures of each of the nine studied alloy samples (samples 10 to 18) from vertical section Sb-CuGe. The observed phases are marked on the micrographs of the alloy samples (Figure 7).
In total, within microstructures of the samples from the Sb-CuGe vertical section four phases were detected: (Ge), (Sb), η(Cu_2Sb) and η'(Cu_3Ge). Hardness of each individual phase was measured according to aforementioned procedure using Vickers test and given as a mean value in Table 9.

Table 9. Measured Vickers micro-hardness of the phases in Sb-CuGe vertical section

Vickers test	Determined phase			
	(Ge)	(Sb)	η(Cu_2Sb)	η'(Cu_3Ge)
hardness (MN/m^2)	855.21	323.87	464.98	518.90

The presented results suggest that the phases rich in Ge have higher hardness. Hardness of the alloy samples was determined by Brinell test and the obtained results are given in Table 10.

Table 10. Brinell hardness of the alloy samples from the Sb-CuGe vertical section

Sample	Mole fraction of components			Brinell hardness (MN/m^2)			
				Value for different measurement			Mean value
	x(Ge)	x(Sb)	x(Cu)	1	2	3	
Bin. 2	0.5	0	0.5	778.6	777.4	774.7	776.9
10	0.45	0.1	0.45	766.5	754.4	744.5	755.1
11	0.4	0.2	0.4	532.3	534.4	537.8	534.8
12	0.35	0.3	0.35	456.5	454.5	457.9	456.3
13	0.3	0.4	0.3	414.2	416.6	419.7	416.8
14	0.25	0.5	0.25	386.7	388.1	389.4	388.1
15	0.2	0.6	0.2	309.4	304.8	308.5	307.6
16	0.15	0.7	0.15	303.5	301.4	308.3	304.4
17	0.1	0.8	0.1	270.3	279.2	278.7	276.1
18	0.05	0.9	0.05	288.6	286.6	287.8	287.7
Ref. [29]	0	1	0	294	-	-	294

According to the obtained results hardness of the samples continually decreases with an addition of Sb. The alloy with the lowest Sb content has higher hardness in comparison to the other alloys from the vertical section and vice versa the alloy with the highest Sb content has the lowest hardness. Graphical presentation of a dependence of hardness of the alloys from Sb content is given on Figure 8.
From Figure 8 it can be seen that the hardness of the alloys decreases with an increase of Sb content. The same alloy samples were used for electrical conductivity measurements and the obtained results are given in Table 11 while graphical presentation is given in Figure 9.

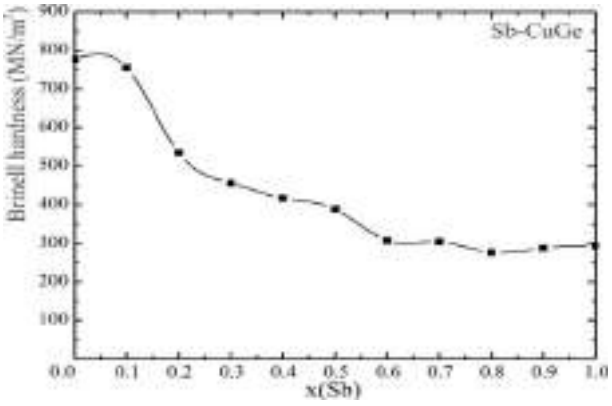

Figure 8. Brinell hardness of the samples from the Sb-CuGe vertical section

D. Gurešić[1], A. Đorđević[1], A. Marković[1], M. Tomović[1], N. Talijan[2], I. Manasijević[3]

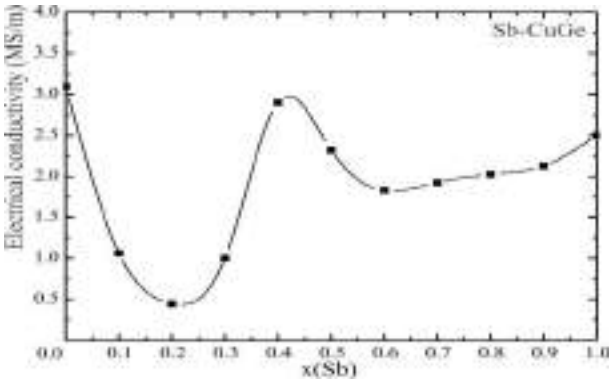

Figure 9. Electrical conductivity of the investigated samples from the Sb-CuGe vertical section

On the presented electrical conductivity vs Sb content curve (Figure 9) three extreme points can be observed. With an increasing Sb content electrical conductivity changes in such manner that it decreases to a minimum for sample 11 and then it increases to a maximum for sample 13 from which it decreases slightly to another minimum for sample 15 and from that point it then continually increases.

Table 11. Electrical conductivity of the alloys from the Sb-CuGe vertical section

Sample	Mole fraction of components			Electrical conductivity MS/m				
				Value for different measurement				Mean value
	x(Ge)	x(Sb)	x(Cu)	1	2	3	4	
Bin. 2	0.5	0	0.5	3.089	3.098	3.098	3.093	3.0945
10	0.45	**0.1**	0.45	1.018	1.015	1.109	1.097	1.0598
11	0.4	**0.2**	0.4	0.453	0.452	0.444	0.434	0.4458
12	0.35	**0.3**	0.35	0.987	1.008	1.002	1.010	1.0018
13	0.3	**0.4**	0.3	2.889	2.913	2.903	2.904	2.9023
14	0.25	**0.5**	0.25	2.318	2.329	2.320	2.320	2.3218
15	0.2	**0.6**	0.2	1.828	1.829	1.826	1.831	1.8285
16	0.15	**0.7**	0.15	1.938	1.912	1.920	1.919	1.9223
17	0.1	**0.8**	0.1	2.027	2.064	2.076	1.937	2.026
18	0.05	**0.9**	0.05	2.123	2.134	2.127	2.125	2.1273
Ref. [27]	0	**1**	0					2.5

On the presented electrical conductivity vs Sb content curve (Figure 9) three extreme points can be observed. With an increasing Sb content electrical conductivity changes in such manner that it decreases to a minimum for sample 11 and then it increases to a maximum for sample 13 from which it decreases slightly to another minimum for sample 15 and from that point it then continually increases.

4.3. Vertical section Cu-GeSb

Nine ternary alloy samples from vertical section Cu-GeSb were investigated using the same experimental techniques as previously studied vertical sections. The alloy samples were labeled with numbers from 19 to 27. The content of Cu in the samples with two consecutive numbers increases for about 10 at. % while contents of Ge and Sb were kept approximately in the same ratio. The obtained results of EDS analysis i.e. compositions of the samples and identified phases are given in Table 12. The obtained results suggest that phase composition of the alloy samples from the vertical section Cu-GeSb changes with an addition of Cu as different phase regions were identified. It was found that within the alloys with Cu content in range ≈ 10 to ≈ 50 at. % Cu three phase regions (Ge)+(Sb)+η(Cu_2Sb) are stable. However, in the samples 24 and 25 other

D. Gurešić[1], A. Đorđević[1], A. Marković[1], M. Tomović[1], N. Talijan[2], I. Manasijević[3]

three phase region was discovered (Ge)+η(Cu_2Sb)+η'(Cu_3Ge). Furthermore, in the sample 26 with 80.34 at. % Cu a third three phase η'(Cu_3Ge)+δ(Cu_4Sb)+ξ(Cu_5Ge) region was found. Still, in the microstructure of the sample 27 only two phase region (Cu)+δ(Cu_4Sb) was detected, which makes the alloy $Cu_{90.06}Ge_{5.07}Sb_{4.87}$ (sample 27) the only one with two phases from all of the studied ternary samples. SEM micrograph illustrating a microstructure of the sample 26 is given on Figure 10. In the microstructure of the alloy sample 26 three intermetallic compounds were detected. Phase δ(Cu4Sb) appears lightest, η'(Cu3Ge) phase is gray and ξ(Cu5Ge) is darkest.

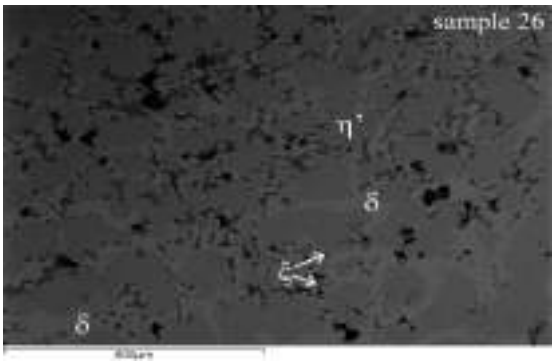

Figure 10. Microstructure of the sample 26 analyzed using SEM-EDS technique

Table 12. Experimentally determined compositions of the samples and phases from Cu-GeSb vertical section

Sample	Overall composition (at.%)	Experiment. Determined phases	Compositions of phases (at.%)		
			Cu	Ge	Sb
			exp.	exp.	exp.
19	10.09 Cu 44.98 Ge 44.93 Sb	(Ge) (Sb) η(Cu_2Sb)	0.32±0.1 0.18±0.2 66.53±0.7	98.79±0.4 0.34±0.1 0.13±0.2	0.89±0.5 99.48±0.8 33.34±0.1
20	20.08 Cu 40.04 Ge 39.88 Sb	(Ge) (Sb) η(Cu_2Sb)	0.53±0.2 0.65±0.2 67.36±0.4	99.12±0.7 0.64±0.4 0.25±0.5	0.35±0.4 98.71±0.3 32.39±0.8
21	30.05 Cu 34.68 Ge 35.27 Sb	(Ge) (Sb) η(Cu_2Sb)	0.76±0.5 0.26±0.3 67.19±0.7	98.90±0.1 0.25±0.2 0.17±0.8	0.34±0.4 99.49±0.4 32.64±0.3
22	39.78 Cu 29.98 Ge 30.24 Sb	(Ge) (Sb) η(Cu_2Sb)	0.37±0.2 0.43±0.2 66.54±0.5	98.68±0.2 0.45±0.4 0.26±0.2	0.95±0.8 99.12±0.3 33.20±0.9
23	50.45 Cu 25.43 Ge 24.12 Sb	(Ge) (Sb) η(Cu_2Sb)	0.83±0.2 0.26±0.8 66.52±0.6	99.03±0.1 0.17±0.1 0.35±0.7	0.14±0.1 99.57±0.2 33.13±0.3
24	60.05 Cu 19.98 Ge 19.97 Sb	(Ge) η(Cu_2Sb) η'(Cu_3Ge)	0.36±0.2 66.54±0.2 75.08±0.6	98.79±0.6 0.26±0.4 24.35±0.5	0.85±0.3 33.20±0.7 0.57±0.2
25	69.67 Cu 15.65 Ge 14.68 Sb	(Ge) η(Cu_2Sb) η'(Cu_3Ge)	0.76±0.4 67.08±0.3 74.67±0.4	98.49±0.2 0.45±0.8 25.19±0.1	0.75±0.8 32.47±0.3 0.14±0.2
26	80.34 Cu 9.98 Ge 9.68 Sb	η'(Cu_3Ge) δ(Cu_4Sb) ξ(Cu_5Ge)	75.45±0.4 80.43±0.5 90.58±0.1	24.46±0.4 0.34±0.3 9.13±0.4	0.09±0.7 19.23±0.6 0.29±0.2
27	90.06 Cu 5.07 Ge 4.87 Sb	(Cu) δ(Cu_4Sb)	95.89±0.2 81.04±0.2	3.98±0.3 0.13±0.7	0.13±0.1 18.83±0.5

D. Gurešić[1], A. Đorđević[1], A. Marković[1], M. Tomović[1], N. Talijan[2], I. Manasijević[3]

The phases identified by EDS were checked by subsequent XRD analysis and the obtained results are given in Table 13 together with experimentally determined values of lattice parameters and corresponding literature data. The obtained results of XRD analysis confirm the phase composition determined by EDS. Determined values of lattice parameters for the phases (Ge), (Sb), η(Cu2Sb) and η'(Cu3Ge) were compared with literature data [24-26, 28] and they were found to be in a close agreement. Three new phases which were detected in the alloy samples 26 and 27 were compared with lattice parameters reported by Schubert et al [30], King et al. [31] and Lejaeghere et al [32]. In this case as well, a very close agreement with literature data was obtained as the observed differences between values were only in the third digit after the decimal point.All of the prepared alloy samples were observed by LOM and microstructures of the four alloy samples 21, 24, 25 and 27 are presented on Figure 11. Three phases can be observed in the microstructure of the sample 21 (Figure 11), two solid solutions and one intermetallic compound. Solid solution (Ge) appears as a gray phase and (Sb) solid solution as a white phase while the intermetallic compound η(Cu_2Sb) appears as a small grain phase. The samples 24 and 25 have almost the same structure, because of the same phase composition (Ge)+η(Cu_2Sb)+η'(Cu_3Ge). The sample 27 consists of two phases, (Cu) and δ(Cu_4Sb) where δ(Cu_4Sb) phase appears as a base phase and solid solution (Cu) as a phase with clearly defined grain boundaries. In total seven different phases were detected in the microstructures of the studied alloy samples from the Cu-GeSb vertical section. Hardness of each phase was determined using Vickers test and the obtained mean values are presented in Table 14.

Table 13. Results of XRD analysis: identified phases and calculated lattice parameters compared with literature data

S.	Coexisting phases		Lattice parameters (Å)					
	SEM-EDS	XRD	a		b		c	
			Exp.	Ref.	Exp.	Ref.	Exp.	Ref.
19	(Ge) (Sb) η(Cu_2Sb)	(Ge) (Sb) η(Cu_2Sb)	5.6578(2) 4.3067(3) 3.9787(3)	5.6522[24] 4.30724[25] 3.97[26]			 11.2734(1) 6.0626(2)	 11.2754[25] 6.06[26]
20	(Ge) (Sb) η(Cu_2Sb)	(Ge) (Sb) η(Cu_2Sb)	5.6576(4) 4.3025(3) 3.9743(2)	5.6522[24] 4.30724[25] 3.97[26]			 11.2735(2) 6.0628(2)	 11.2754[25] 6.06[26]
21	(Ge) (Sb) η(Cu_2Sb)	(Ge) (Sb) η(Cu_2Sb)	5.6537(2) 4.3098(2) 3.9745(2)	5.6522[24] 4.30724[25] 3.97[26]			 11.2756(2) 6.0687(3)	 11.2754[25] 6.06[26]
22	(Ge) (Sb) η(Cu_2Sb)	(Ge) (Sb) η(Cu_2Sb)	5.6525(3) 4.3035(2) 3.9746(2)	5.6522[24] 4.30724[25] 3.97[26]			 11.2798(5) 6.0639(3)	 11.2754[25] 6.06[26]
23	(Ge) (Sb) η(Cu_2Sb)	(Ge) (Sb) η(Cu_2Sb)	5.6535(2) 4.3098(1) 3.9768(2)	5.6522[24] 4.30724[25] 3.97[26]			 11.2739(2) 6.0687(7)	 11.2754[25] 6.06[26]
24	(Ge) η(Cu_2Sb) η'(Cu_3Ge)	(Ge) η(Cu_2Sb) η'(Cu_3Ge)	5.6538(2) 3.9786(3) 5.2748(7)	5.6522[24] 3.97[26] 5.272[28]	 4.2078(6)	 4.204[28]	 6.0687(2) 4.5785(4)	 6.06[26] 4.578[28]
25	(Ge) η(Cu_2Sb) η'(Cu_3Ge)	(Ge) η(Cu_2Sb) η'(Cu_3Ge)	5.6538(2) 3.9786(4) 5.2786(3)	5.6522[24] 3.97[26] 5.272[28]	 4.2089(2)	 4.204[28]	 6.0644(5) 4.5727(3)	 6.06[26] 4.578[28]

26	η' (Cu_3Ge) δ(Cu_4Sb) ξ (Cu_5Ge)	η' (Cu_3Ge) δ(Cu_4Sb) ξ (Cu_5Ge)	5.2786(4) 2.7528(8) 2.5987(4)	5.272[28] 2.752[30] 2.5923[31]	4.2045(3)	4.204[28]	4.5729(4) 4.3289(6) 4.2289(4)	4.578[28] 4.320 [30] 4.2247 [31]
27	(Cu) δ(Cu_4Sb)	(Cu) δ(Cu_4Sb)	3.6398(7) 2.7587(3)	3.63689 [32] 2.752[30]			4.3298(6)	4.320 [30]

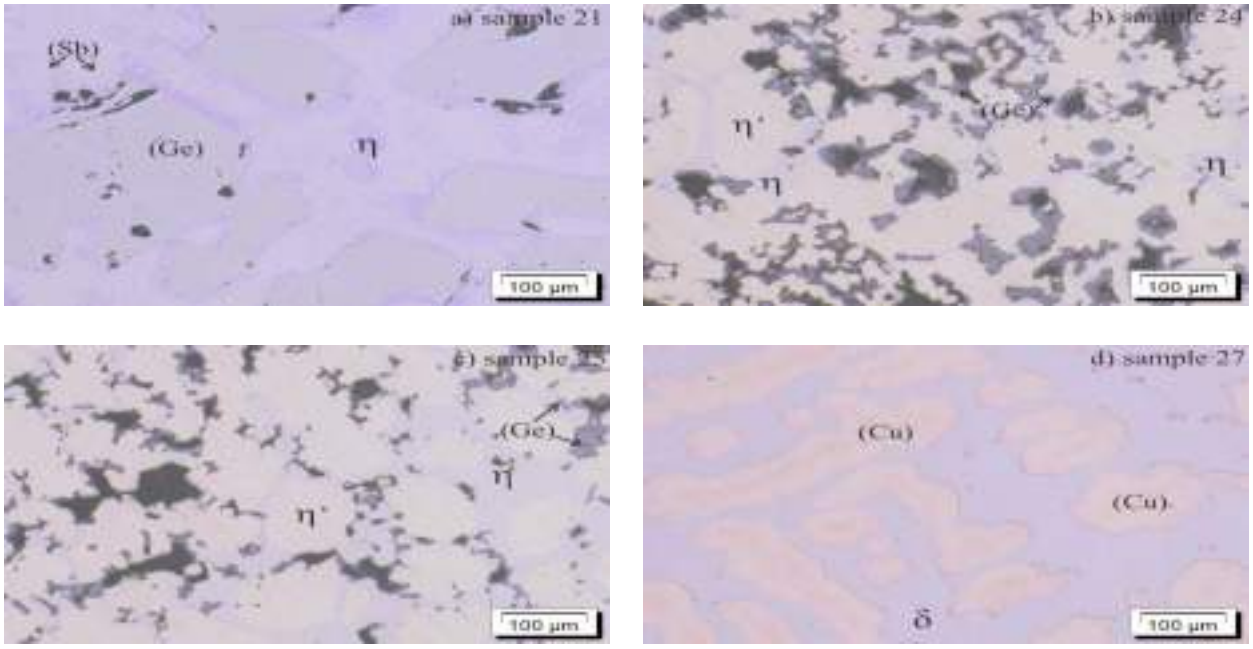

Figure 11. Microstructures of the selected alloy samples observed with LOM

Table 14. Measured Vickers micro-hardness of the phases from the Cu-GeSb vertical section

Vickers test	Determined phase						
	(Ge)	(Sb)	η(Cu_2Sb)	η'(Cu_3Ge)	δ(Cu_4Sb)	ξ (Cu_5Ge)	(Cu)
hardness (MN/m^2)	858.29	336.13	454.98	513.71	603.16	745.3	944.18

The obtained results suggest that hardness of the individual phases increases with an increase of Cu content. Hence, the solid solution (Cu) has the highest hardness from all of the identified phases in the ternary Cu-Ge-Sb system, whereas the solid solution (Sb) has the lowest. Experimentally determined values of Brinell hardness of the studied alloy samples are given in Table 15.

D. Gurešić[1], A. Đorđević[1], A. Marković[1], M. Tomović[1], N. Talijan[2], I. Manasijević[3]

Table 15. Brinell hardness of the alloys from the Cu-GeSb vertical section

Sample	Mole fraction of components			Brinell hardness (MN/m^2)			
				Value for different measurement			Mean value
	x(Ge)	x(Sb)	x(Cu)	1	2	3	
Bin. 3	0.5	0.5	0	345.8	346.1	345.1	345.6667
19	0.45	0.45	0.1	389.7	398.7	392.1	393.5
20	0.4	0.4	0.2	360.8	355.4	350.9	355.7
21	0.35	0.35	0.3	340.6	345.6	343.6	343.2667
22	0.3	0.3	0.4	378.9	376.4	379.5	378.2667
23	0.25	0.25	0.5	420.5	423.3	422.3	422.0333
24	0.2	0.2	0.6	498.7	503.6	505.6	502.6333
25	0.15	0.15	0.7	644.5	643.4	645.8	644.5667
26	0.1	0.1	0.8	698.9	703.5	706.7	703.0333
27	0.05	0.05	0.9	765.6	767.4	765.7	766.2333
Ref. [29]	0	0	1	874	-	-	874

Graphical presentation of a relation between Brinell hardness of the alloys from the studied Cu-GeSb vertical section and Cu molar content is given on Figure 12. From Figure 12 it can be seen that the sample 21 has the lowest hardness of the alloys of Cu-GeSb vertical section. Starting from the sample 21, hardness of the alloys increases both with an increase and a decrease of Cu molar content. Measured values of electrical conductivity of the studied alloy samples are given in Table 16. The presented values represent an average of four measurements.

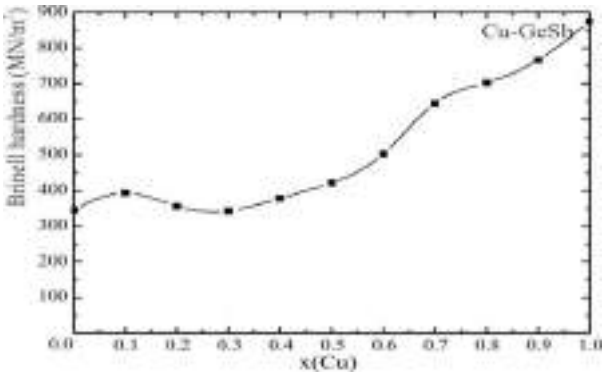

Figure 12. Brinell hardness of the alloy samples from the Cu-GeSb vertical section

Graphical presentation of a dependence of electrical conductivity of the studied alloy samples on molar content of Cu is given on Figure 13.

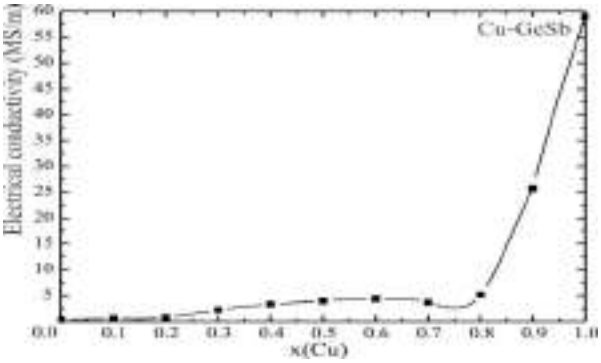

Figure 13. Electrical conductivity of the investigated alloy samples from the Cu-GeSb vertical section

From Figure 13 and Table 16 it can be seen that electrical conductivity increases with an increasing content of Cu. Slight inconsistency with this trend can be observed for the sample 25 whereas the sample 27 has the highest electrical conductivity from all of the other studied samples from the ternary Cu-Ge-Sb system.

D. Gurešić[1], A. Đorđević[1], A. Marković[1], M. Tomović[1], N. Talijan[2], I. Manasijević[3]

Table 16. Electrical conductivity of the alloys from the Cu-GeSb vertical section

Sample	Mole fraction of components			Electrical conductivity MS/m				
				Value for different measurement				Mean value
	x(Ge)	x(Sb)	x(Cu)	1	2	3	4	
Bin. 3	0.5	0.5	0	0.343	0.341	0.353	0.344	0.3453
19	0.45	0.45	0.1	0.535	0.536	0.539	0.538	0.537
20	0.4	0.4	0.2	0.714	0.712	0.745	0.736	0.7268
21	0.35	0.35	0.3	2.180	2.189	2.180	2.183	2.183
22	0.3	0.3	0.4	3.276	3.560	3.233	3.213	3.3205
23	0.25	0.25	0.5	3.989	3.988	3.989	4.009	3.9938
24	0.2	0.2	0.6	4.494	4.502	4.172	4.439	4.4018
25	0.15	0.15	0.7	3.543	3.567	3.598	3.989	3.6743
26	0.1	0.1	0.8	2.004	2.013	1.997	2.002	5.1905
27	0.05	0.05	0.9	5.156	5.200	5.201	5.205	25.7351
Ref. [27]	0	0	1					59

4.4. Mathematical calculation of electrical conductivity and hardness

Based on the experimentally obtained results and using suitable mathematical model, values of hardness and electrical conductivity along the whole composition range were predicted.
For this calculation the software package Desig Expert v.9.0.3.1 and canonical or Scheffe model [33-35] were used. For calculation of iso-lines of Brinell hardness Special Quartic model was selected and the final equation of the predictive model in terms of actual components is:

$$HB\ (MN/m^2) = 821.76507 \cdot x(Ge) + 268.39142 \cdot x(Sb) + 830.24943 \cdot x(Cu) - 766.46391 \cdot x(Ge) \cdot x(Sb) + 35.98254 \cdot x(Ge) \cdot x(Cu) - 718.80424 \cdot x(Sb) \cdot x(Cu) - 13424.42258 \cdot x(Ge)^2 \cdot x(Sb) \cdot x(Cu) + 7546.76969 \cdot x(Ge) \cdot x(Sb)^2 \cdot x(Cu) \quad (1)$$

Iso-lines contour plot of Brinell hardness of alloys defined by equation 1 is shown on Figure 14.

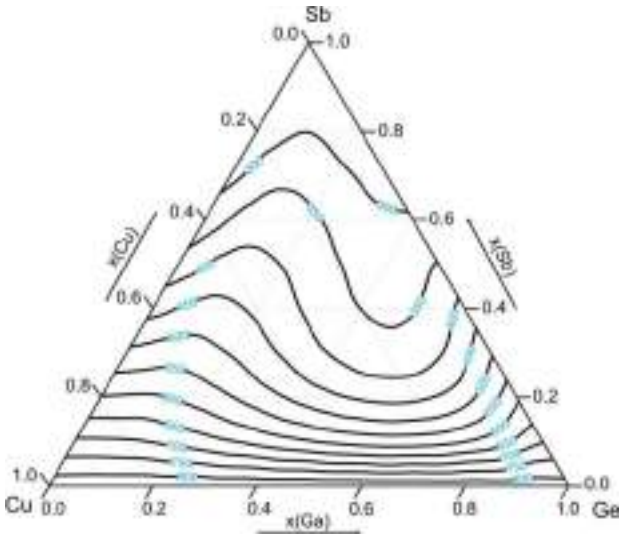

Figure 14. Iso-lines of Brinell hardness of alloys of the ternary Cu-Ge-Sb system

D. Gurešić[1], A. Đorđević[1], A. Marković[1], M. Tomović[1], N. Talijan[2], I. Manasijević[3]

Calculation of electrical conductivity of the alloys from the Cu-Ge-Sb ternary system was carried out in the same manner as the aforementioned Brinell hardness calculation.

Model summary statistics are suggested Special Quartic. The final equation of the predictive model in terms of actual components is:

$$\sigma\ (MS/m) = -4.01695 \cdot x(Ge) + 0.72495 \cdot x(Sb) + 3.6745 \cdot x(Cu) + 3.13539 \cdot x(Ge \cdot x(Sb) + 5.55345 \cdot x(Ge) \cdot x(Cu) - 2.83122 \cdot x(Sb) \cdot x(Cu) + 17.95432 \cdot x(Ge)^2 \cdot x(Sb) \cdot x(Cu) + 30.80395 \cdot x(Ge) \cdot x(Sb)^2 \cdot x(Cu) - 79.8965 \cdot x(Ge) \cdot x(Sb) \cdot x(Cu)^2 \quad (2)$$

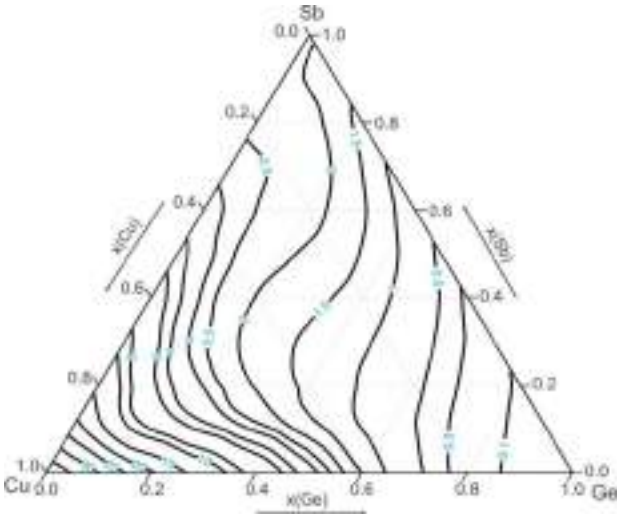

Figure 15. Iso-lines of electrical conductivity of alloys of the ternary Cu-Ge-Sb system

The obtained iso-lines contour plot of electrical conductivity defined by equation 2 is shown on Figure 15.

5. CONCLUSION

Twenty-seven ternary alloys from three vertical sections (Cu-GeSb, Ge-CuSb and Sb-CuGe) of the Cu-Ge-Sb system were experimentally investigated using LOM, SEM-EDS, XRD, Brinell and Vickers hardness tests and electrical conductivity measurements. Chemical compositions and compositions of phases determined using EDS analysis demonstrate that apart from several alloys that build slightly different three phase regions such as (Ge)+η(Cu_2Sb)+η'(Cu_3Ge) and η'(Cu_3Ge)+δ(Cu_4Sb)+ξ(Cu_5Ge) and only one that builds δ(Cu_4Sb)+(Cu) two phase region, the majority of the studied alloy samples build the same (Ge)+(Sb)+η(Cu_2Sb) three phase region. It was found that the solubility of the third element into the intermetallic compound was less than 1 at. % as well as that the solubility of Sb and Cu into (Ge) solid solution is also very low and that the same is true for solid solution (Sb). Experimentally determined solubility Ge of 3.98 at.% in the solid solution (Cu) is within the plausible range as according to literature the solid solution (Cu) can dissolve maximum ≈ 11.5 at.% of Ge. The determined phase compositions were confirmed with XRD analysis and observed with light optical microscopy. Besides confirmation of the phase regions, XRD analysis has also provided crystal lattice parameters of the detected phases. As an additional confirmation, the calculated lattice parameters were found to be in a close agreement with literature data.

The obtained results of Vickers hardness test show that out of the seven different phases that were identified in the Cu-Ge-Sb system, the (Cu) phase has the highest hardness, followed by (Ge), ξ (Cu_5Ge), δ(Cu_4Sb), η'(Cu_3Ge), η(Cu_2Sb) and (Sb) in a descending order. According to the results of Brinell hardness and electrical conductivity measurements the alloys from Cu-GeSb vertical section exhibit stable and continual increase of values of both properties with an increase of Cu content. Hence, it can be concluded that the alloy with highest amount of Cu has both the highest hardness and electrical conductivity.

Based on the obtained experimental results and mathematical calculations iso-lines of Brinell hardness and electrical conductivity were calculated for the whole Cu-Ge-Sb system. The calculated iso-lines can give information on Brinell hardness and electrical conductivity of all possible ternary Cu-Ge-Sb alloys

Acknowledgements

This work was supported by the Ministry of Education, Science and Technological Development of the Republic of Serbia, under Project No. ON172037.

REFERENCES

[1] Cui, S. L.. Zhang, L. J.. Zhang, W. B.. Du, Y.. Xu, H. H.. (2012). Computational study of diffusivities in diamond Ge-Si alloys. Journal of Mining and Metallurgy, Section B, 48(2), 227-249.

[2] Amore, S.. Giuranno, D.. Novakovic, R.. Ricci, E.. Nowak, R.. Sobczak, N.. (2014). Thermodynamic and surface properties of liquid Ge–Si alloys. Calphad, 44, 95-101.

[3] Jin, S.. Leinenbach, C.. Wang, J.. Duarte, L. I.. Delsante, S.. Borzone, G.. Scott, A.. Watson, A.. (2012). Thermodynamic study and re-assessment of the Ge-Ni binary system. Calphad, 38, 23-34.

[4] Kazemi, H.. Weber, L.. (2012). Solid solubility of germanium in silver. Thermochimica Acta, 544, 57-62.

[5] Kostov, A.. Zivkovic, D.. Zivkovic, Z.. (2000). Comparative thermodynamic analysis of Ga-GeSb0.855 section in the ternary system Ga-Ge-Sb. Journal of thermal analysis and calorimetry, 60, 473-487.

[6] Gandova, V.. Lilova, K.. Malakova, H.. Huber, B.. Milcheva, N.. Ipser, H.. Vrestal, J.. Vassilev, G.. (2010). On the synthesis of Bi–based precursors for lead-free solders development. Journal of Mining and Metallurgy, Section B, 46(1), 11-23.

[7] Liu, C. P.. Hsu, C. C.. Jeng, T. R.. Chen, J. P.. (2009). Enhancing nanoscale patterning on Ge-Sb-Sn-O inorganic resist film by introducing oxygen during blue laser-induced thermal lithography. Journal of Alloys and Compounds, 488, 190-194.

[8] Chawanda, A.. Nyamhere, C.. Auret, F.D.. Mtangi, W.. Diale, M.. Nel, J.M.. (2010). Thermal annealing behaviour of platinum, nickel and titanium Schottky barrier diodes on n-Ge (100). Journal of Alloys and Compounds, 492, 649-655.

[9] Zarembo, S. N.. Myers, C. E.. Kematick, R. J.. Zavalij, P. Y.. Whittingham, M. S.. Cotts, E. J.. (2001).Journal of Alloys and Compounds, 329, 97-107.

[10] Kanibolotsky, D. S.. Kotova, N. V.. Bieloborodova, O. A.. Lisnyak, V. V.. (2003). Thermodynamics of liquid aluminium–copper–germanium alloys. The Journal of Chemical Thermodynamics, 35, 1763-1774.

[11] Ielmini, D.. Lacaita, A. L.. (2011). Phase change materials in non-volatile storage. Materials Today, 14(12), 600-607.

[12] Wełnic, W.. Wuttig, M.. (2008). Reversible switching in phase-change materials. Materials Today, 11 (6), 20-27.

[13] Raoux, S.. Shelby, R. M.. Jordan-Sweet, J.. Munoz, B.. Salinga, M.. Chen, Y. C.. Shih, Y. H.. Lai, E. K.. Lee, M. H.. (2008). Phase change materials and their application to random access memory technology. Microelectronic Engineering, 85, 2330-2333.

[14] Bahgat, A. A.. Mahmoud, E. A.. Abd Rabo, A. S.. Mahdy, I. A.. (2006). Study the physical and ferroelectric properties of some Ge-Sb-Te alloys. Physics, 382, 271-278.

[15] Caldwell, M. A.. Gnana David Jeyasingh, R.. Philip Wong, H. S.. Milliron, D. J.. (2012). Nanoscale phase change memory materials. Nanoscale, 4, 4382-4392.

[16] Jin, S.. Duarta, L. I.. Leinenbach, C.. (2014). Experimental study and thermodynamic description of the Au-Cu-Ge system. Journal of Alloys and Compounds, 588, 7-16.

[17] Ruan, Y.. Wang, X. J.. Lu, X. Y.. (2013). Pseudobinary eutectics in Cu–Ag–Ge alloy droplets under containerless condition. Journal of Alloys and Compounds, 563 85-90.

[18] Premovic, M.. Minic, D.. Cosovic, V.. Manasijevic, D.. Zivkovic, D.. (2014) Experimental investigation and thermodynamic calculations of the Bi-Ge-Sb phase diagram. Metallurgical and materials transactions A -Physical metallurgy and materials science, 45a, 4829-4841

[19] Premovic, M.. Manasijevic, D.. Minic, D.. Zivkovic, D.. (2014). Experimental investigation and thermodynamic prediction of the Ag-Ge-Sb phase diagram. Journal of Alloys and Compounds, 610, 161-168

[20] Premovic, M.. Manasijevic, D.. Minic, D.. Zivkovic, D.. (2014). Experimental investigation and thermodynamic calculation of the Ge-In-Sb phase diagram, Materials chemistry and physics, 148, 356-363

[21] Wang, J.. Jin, S.. Leinenbach, C.. Jacot, A.. (2010). Thermodynamic assessment of the Cu–Ge binary system. Journal of Alloys and Compounds, 504, 159-165.

[22] Liu, J.. Guo, C.. Li, C.. Du, Z.. (2011). Thermodynamic Optimization of the Ge-Sb and Ge-Sb-Sn Systems. Thermochimica Acta, 520, 38-47.

[23] Liu, X. J.. Wang, C.P.. Ohnuma, I.. Kainuma, R.. Ishida, K.. (2000). Thermodynamic assessment of the phase diagrams of the Cu-Sb and Sb-Zn systems. Journal of phase equilibria, 21, 432-442.

[24] Morozkin, A. V.. (2012). Gd - Co - Ge system at 870/1070 K. Intermetallics 25 136-138.

[25] Li, J. Q.. Feng, X. W.. Sun, W. A.. Ao, W. Q.. Liu, F. S.. Du, Y.. (2008). Solvothermal synthesis of nano-sized skutterudite Co4-x Fex Sb12 powders, Materials Chemistry and Physics, 112, 57-62.

[26] Reshak, A. H.. Kamarudin, H.. (2011). Theoretical investigation for Li2 Cu Sb as multifunctional materials: electrode for high capacity rechargeable batteries and novel materials for second harmonic generation. Journal of Alloys and Compounds, 509(30), 7861-7869.

[27] http://periodictable.com/Properties/A/ElectricalConductivity.an.html, accesses 27.06.2016.

[28] E. Caspi, H. Shaked, H. Pinto, M. Melamud, Z. Hu, O. Chmaissem, S. Short, J. D. Jorgensen, J. Alloys Compd. 271 (1998) 378-381.

[29] http://www.webelements.com/periodicity/hardness_brinell/, accesses 27.06.2016.

[30] Schubert, K.. Breimer, H.. Burkhardt, W.. Gunzel, E.. Haufler, R.. Lukas H. L.. Vetter, H.. Wegst, J.. Wilkens, M.. (1957). Einige strukturelle Ergebnisse an metallischen Phasen. II. Naturwissenschaften, 44(7), 229-230.

[31] King, H. W.. Massalski, T. B.. Isaacs, L. L.. (1963). Axial ratio changes in H.C.P. zeta phases in the systems Au - In - Cu and Cu - Ge – Au. Acta Metallurgica, 11, 1355-1361.

[32] Lejaeghere, K.. Van Speybroeck, V.. Van Oost, G.. Cottenier, S.. (2014). Error estimates for solid-state density-functional theory predictions: an overview by means of the ground-state elemental crystals. Reviews in Solid State and Materials Sciences, 39(1), 1-24

[33] Cornell: Experiments with Mixtures,3rd Ed., John Wiley&Sons, Inc, New York (2002)

[34] Lazić, Ž. Design of Experiments in Chemical Engineering, Wilez-VCH Verlag GmbH&Co.KGaA, Weiheim (2004).

[35] Kolarević, M.. Vukićević, M.. Radičević, B.. Bjelić, M.. Grković, V.. The Seventh Triennial International Conference Heavy Machinery HM 2011, 29.06-02.07. Vrnjačka Banja (2011), pp. 1-